Available online at www.sciencedirect.com
SCIENCE DIRECT
International Journal of Fatigue 27 (2005) 1179–1185
International Journal of Fatigue
www.elsevier.com/locate/ijfatigue

Fatigue damage in nickel and copper single crystals at nanoscale

G.P. Potirniche[a,*], M.F. Horstemeyer[a], B. Jelinek[a], G.J. Wagner[b]

[a]Center for Advanced Vehicular System, Mississippi State University, Box 5405, Mississippi State, MS 39762, USA
[b]Sandia National Laboratories, Livermore, CA, USA

Available online 20 July 2005

Abstract

Nanoscale fatigue damage simulations using molecular dynamics were performed in nickel and copper single crystals. Cyclic stress–strain curves and fatigue crack growth were investigated using a middle-tension (MT) specimen with the lateral sides allowing periodic boundary conditions to simulate a small region of material as a part of a larger component. The specimen dimensions were in the range of nanometers, and the fatigue loading was strain controlled under constant and variable amplitude. Four crystal orientations, [111], [100], [110] and [101] were analyzed, and the results indicated that the plastic deformation and fatigue crack growth rates vary widely from one orientation to another. Under increasing strain amplitude loading, nickel nanocrystals experienced a large amount of plastic deformation causing at least in one orientation, [101], out-of-plane crack deviation in a mixed mode I+ II growth. Under constant amplitude loading, the fatigue cracks were a planar mode I type. Double slip is observed for some orientations, while for others, many more slip systems were activated causing a more evenly distributed plastic region around the crack tip. A comparative analysis revealed that small cracks grow more rapidly in copper than in nickel single crystals.

Keywords: Persistent slip bands; Fatigue crack growth; Nickel; Copper; Single crystal; Molecular dynamics

1. Introduction

Due to the advances in manufacturing technologies of nano-materials there is a growing need for computational models of mechanical behavior at very small length scales. Fatigue damage within single crystals at nanoscale is an outstanding issue for researchers and designers. Studies that previously dealt with various aspects of fatigue damage in single crystals at microstructural length scales must be extended at the smaller, atomistic, length scale. Numerous macroscopic experimental accounts exist of such phenomena in nickel and copper single crystals.

Cyclic behavior in copper single crystals has been extensively researched. Fatigue damage in copper single crystals is indicated by the formation of persistent slip bands (PSB) and consequent nucleating cracks [1–4], hardening saturation of the stress–strain cyclic curve [5,6], and strain bursts [7]. Jin [3] analyzed the formation of persistent slip bands (PSB) and vein structures in fatigued single crystals of copper oriented for double slip, and he found a strong dependence on the orientation of the formation of either fairly uniform (ladder-like) cell walls structures or matrix vein structures. Mughrabi [6] indicated that no PSB are formed below a threshold value of applied strain implying a fatigue limit in copper, and underscored the role of internal stresses in the formation and evolution of PSB. By using an orientation favorable for single slip, Zhang [8] described two types of dislocation bands in fatigued copper, slip bands with little plastic deformation and deformation bands that sustained large plastic deformation. Basinski et al. [9] investigated the details of plastic deformation in the slip bands and observed that plastic slip within the PSB is nonuniform, with local strain at least one order of magnitude larger than the constant strain in the PSB. Lorenzo [7] explained that during fatigue loading dislocation locking can occur in copper single crystals, and these can subsequently collapse causing the commonly known phenomenon of strain bursts.

Buque [10] examined the cyclic behavior and dislocation patterns at room temperature in nickel single crystals oriented along directions [011] and [$\bar{1}$11], and he also observed that in nickel single crystals the most prolific phenomenon were the PSB in the orientation [011]. Studies by Bhat and Laird [11,12] of cyclic deformation behavior of

* Corresponding author. Tel.: +1 662 325 5571; fax: +1 662 325 5443.
E-mail address: gabriel@cavs.msstate.edu (G.P. Potirniche).

0142-1123/$ - see front matter © 2005 Elsevier Ltd. All rights reserved.
doi:10.1016/j.ijfatigue.2005.06.015

nickel at high temperatures revealed that a saturation of the stress–strain curve arose.

In the past years advances have been made in the modeling of single crystals using crystal plasticity theory. This theory, which is a kinetics-based deformation theory accounting for the anisotropic nature of plastic slip in single crystals cast into a continuum mechanics kinematics framework, has been successful in modeling plastic strain localization, lattice reorientation, and stress–strain behavior under monotonic loading. However, many of the hardening laws used in the constitutive theory of crystal plasticity are empirical in nature. Also, little work has been done in analyzing cyclic behavior of single crystals using crystal plasticity theory. In addition to crystal plasticity, an insightful tool for studying the mechanics of deformation within single crystals is molecular dynamics. This theory is essentially of discrete mechanics nature, because the single crystal is represented by the collection of individual atoms forming the crystalline lattice. In fracture studies molecular dynamics has been little used. Shen [13] analyzed the ductile fracture behavior of a single crystal with the plastic deformation nucleating from a small interstitial defect using molecular dynamics with Morse pair-wise potential. Fracture and fatigue behavior of nanoscale in single and polycrystal iron was performed using molecular dynamics by Inoue et al. [14]. They found that the tensile strength in polycrystals is smaller than in single crystals due mainly to the propagation of cracks at grain boundaries. Heino et al. [15] used molecular dynamics to simulate the crack nucleation and propagation during ductile fracture measured the dislocation propagation velocity and crack propagation velocity in copper.

In this study we analyzed the fatigue damage by PSB formation and the cyclic stress–strain behavior in nickel single crystal as well as the fatigue crack growth in an MT specimen of nickel and copper, respectively. The influence of lattice orientation was also analyzed by considering four significant directions on the basic stereographic triangle. Finally, a comparative study between the fatigue crack growth in nickel and copper single crystals is undertaken.

2. Computational model and crystal orientations

The computational method used in this study to implement the constitutive response of single crystals at the nanoscale is the Modified Embedded Atom Method (MEAM) potentials [16–18]. The MEAM potential is based on molecular dynamics principles developed initially by Daw and Baskes [19]. MEAM allows the calculation of the thermodynamic forces and stress tensors for the atoms in the lattice based on the notion of embedded energy. Atomistic simulations were shown to give results that agree well with the phenomenological attributes of plasticity observed in macroscale experiments [20].

To study the cyclic stress–strain response and fatigue crack growth, an MT specimen was employed and is shown in Fig. 1a. The dimensions of the specimen given in atomic lattice distance are also given in Fig. 1a. For orientations A, C and D, the dimensions of the specimens specified in Fig. 1a were rounded off to account for the lattice rotation. The specimen sizes were chosen large compared with the crack length ($2H/a = 100$, $W/a = 20$), so that the edge effects are eliminated for most of the crack growth of interest. The loading was applied in the y direction and the specimens were assigned geometric periodicity in the x and z directions. The results concerning the cyclic stress–strain curves were obtained using the specimen illustrated in Fig. 1a, but the crack was replaced by a small circular void with a diameter equal to the crack length necessary to initiate plastic slip. The loading axis was aligned with one of the crystal directions A [111], B [100], C [110], or D [101], as indicated in Fig. 1b. This figure also shows the calculated Schmid factors for each orientation. The largest Schmid factor is 0.408 for orientations B, C, and D, and the smallest is 0.272 on orientation A. The specimens were built using an fcc lattice, and the resulting number of atoms ranged from 148,308 for orientation C to 218,216 for orientation E.

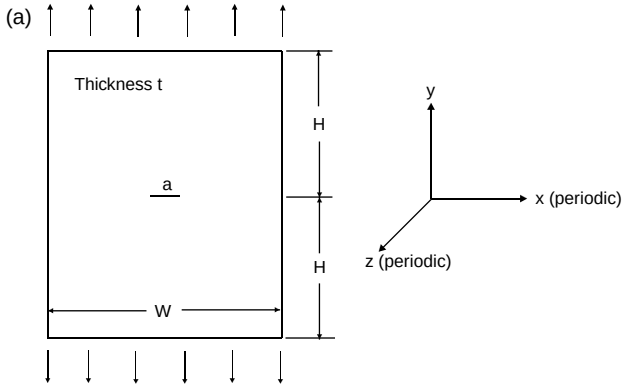

Specimen dimensions
(for *Ni*, d = 0.352 nm, for *Cu*, d = 0.362 nm)

H	W	a	t
50d	100d	5d	4d

MT specimen

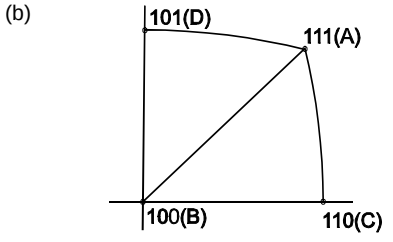

Schmid factors and number of atoms in the specimen
for orientations A-D

A	B	C	D
0.272	0.408	0.408	0.408
182,368	152,692	148,308	218,216

Crystal orientations

Fig. 1. M(T) specimen used for fatigue crack growth simulations.

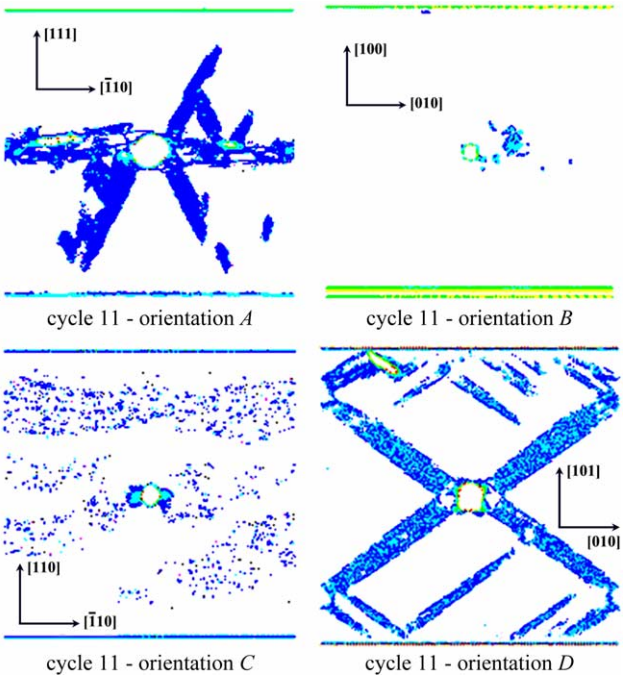

Fig. 2. Plastic slip patterns in nickel single crystal near a small circular void during fatigue loading at constant strain amplitude with $\varepsilon_{max}=0.005$ and $\varepsilon_{min}/\varepsilon_{max}=0.5$. All plots were taken at a 0.0045 applied strain during unloading, except the plot for orientation *B* that was taken during loading.

The model temperature at which the simulations were performed was 300 K.

3. Fatigue damage by persistent slip bands around a small circular void

Dislocation structure during fatigue loading at constant strain amplitude was analyzed, and the main results are presented in Figs. 2 and 3. The fatigue loading applied had a maximum strain of $\varepsilon_{max}=5\times10^{-3}$ and a ratio of $R=\varepsilon_{min}/\varepsilon_{max}=0.5$. The high load ratio was chosen in order to prevent the inner faces of the void from contacting each other during unloading. From previous simulations, it was observed that contact of the crack surfaces leads to the gluing of the crack faces and difficulty in propagating the crack. All the specimens were cyclically loaded up to 11 cycles at which point the simulations were stopped. Fig. 2 presents the dislocation structures observed during the cyclic loading. These patterns vary widely from one orientation to another. In the case of orientation *A* [111] crystallographic direction, the nickel single crystal experienced a triple slip pattern with the three main shear bands nucleating from the small circular void. One of the shear bands aligned with the *x* direction, corresponding to [$\bar{1}$10] direction, while the other two shear

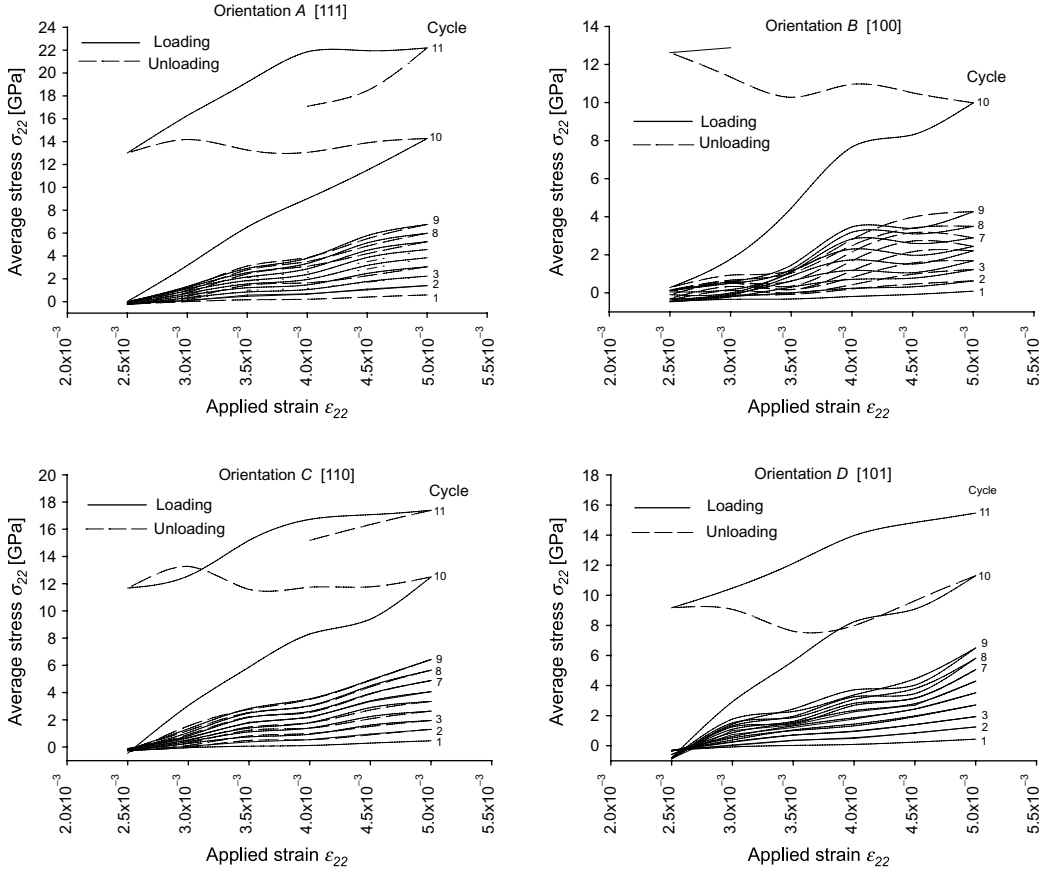

Fig. 3. Cyclic stress–strain curves for the nickel specimens indicated in Fig. 1. The loading was cyclic at constant strain amplitude with $\varepsilon_{max}=0.005$ and $\varepsilon_{min}/\varepsilon_{max}=0.5$.

bands were positioned symmetrically about the [111] direction (y axis). In the case of orientation B, with the loading in the [100] direction, practically very little plastic deformation is experienced by the single crystal, and the slip is localized near the void. Orientation C [110] indicates that the dislocations are organized in vein-like structures in some parallel bands along the $[\bar{1}10]$ direction, very similar to the dislocation structures observed experimentally by Zhang [8]. In the case of orientation D, with loading applied in the [101] direction, the crystal experienced a double slip pattern. Most plastic deformation in this orientation is localized in the shear bands emanating from the void. Smaller voids and crack-like voids are nucleated in the vicinity of the main void as a result of the intense plastic deformation in the shear bands, phenomenon also observed experimentally by Zhang [8]. The cyclic stress–strain curves for the first 11 cycles are shown in Fig. 3. A dominant feature of all orientations is that for the first 9 cycles, the plastic deformation is very small, but still noticeable in the change of the overall slope of the stress–strain curve and some plastic energy dissipated during the hysteresis loops of loading and unloading each cycle. For all orientations, beginning with cycle 10, a sudden increase in the slope of the stress–strain curve is observed, as a result of the plastic strain localization in dislocations bands. Nickel single crystal in orientation A exhibiting triple slip structure indicated the largest stress 14 GPa in cycle 10 at the peak strain in the cycle of 5×10^{-3}. The smallest stress is exhibited by orientation B to about 9.9 GPa in cycle 10. From Fig. 3 it can be concluded that after the first fatigue cycles, the onset of significant plastic deformation occurs very suddenly with a stress burst during the 10th loading cycle. The crystal orientation determines the configuration of dislocation structures in the shear bands, but it has no influence on the cycle at which the single crystal experiences the first large increase in stress hardening.

4. Fatigue crack growth under increasing strain amplitude

The MT specimen shown in Fig. 1 was loaded with increasing strain amplitude fatigue loading indicated in Fig. 4. Under increasing strain amplitude the initial crack with length $a=d$ (atomic lattice distance) propagated very rapidly, and in only 3 cycles the crack reached the edge. The snapshots of the fatigue crack presented in Fig. 2 indicate that the intense plastic slip near the crack tip causes the crack to extend; however, different orientations present a different mechanism of crack extension. Orientation A, indicates that the crack is initially extended isotropically, becoming more of a void due to the intense plastic deformation bands positioned symmetrically with respect to the vertical [111] direction. Orientation B, indicates that the initial crack grows almost parallel with the horizontal direction [010] and with notable crack tip blunting. In the case of this orientation, the plastic zone at the crack tip is somehow uniformly spread around the crack tip. Orientation C shows the initial crack growing very flatly along the $[\bar{1}10]$ horizontal direction. The crack tip does not show much blunting as in the previous case of orientation B. Orientation D experienced initially a crack growing perpendicular to the loading direction as a mode I crack. Then, the intense double slip pattern of deformation at the crack tip causes void formation in the shear bands and consequent deviation of the crack out of the horizontal [010] plane. Further, the crack propagates in a mixed mode I+ II along one of the main shear bands from this point.

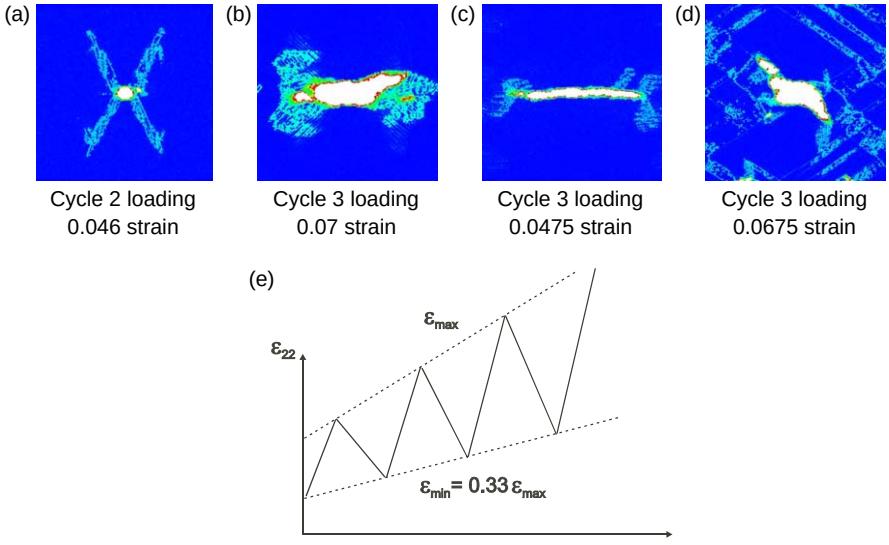

Fig. 4. Fatigue crack growth under variable strain amplitude in nickel single crystals for orientations (a) A[111], (b) B[100], (c) C[110], (d) D [101], and (e) loading cycles with increasing strain amplitude applied to the MT specimen.

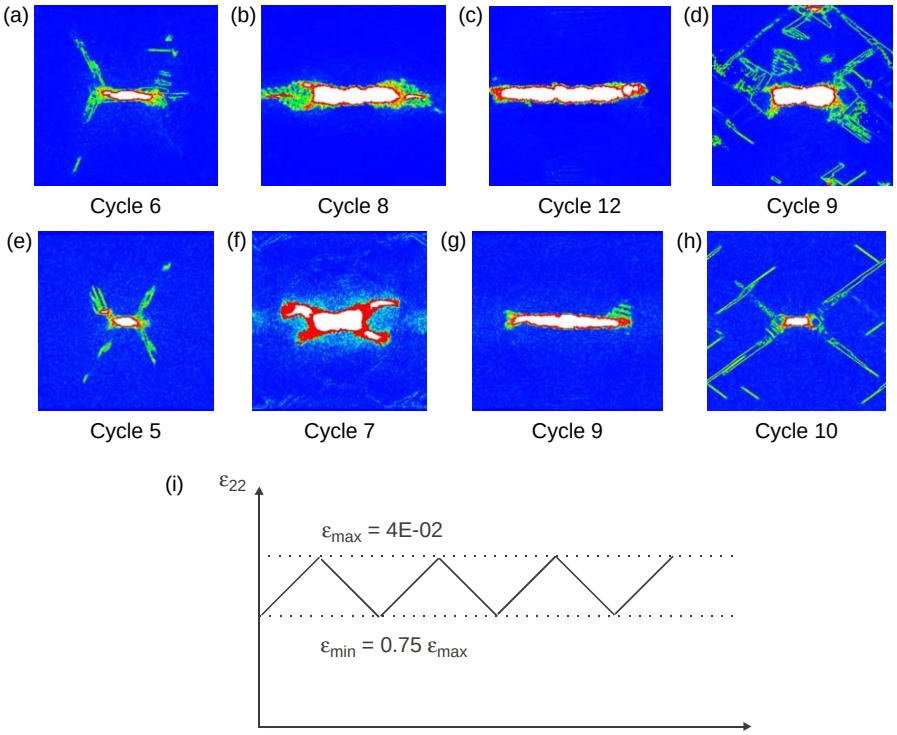

Fig. 5. Fatigue crack growth under variable strain amplitude in nickel and copper single crystals for orientations (a) Ni, *A*[111]; (b) Ni, *B*[100]; (c) Ni, *C*[110]; (d) Ni, *D* [101]; (e) Cu, *A*[111]; (f) Cu, *B*[100]; (g) Cu, *C*[110]; (h) Cu, *D* [101], and (i) fatigue loading with constant strain amplitude applied to the MT specimen from Fig. 1.

5. Fatigue crack growth under constant strain amplitude

Constant strain amplitude loading was also analyzed using both nickel and copper single crystals. The maximum applied strain in the fatigue cycle was 4×10^{-2} with a ratio of 0.75. The high load ratio was necessary to keep the crack planes from contacting each other. Fig. 5a–d presents the contour plots of the deformational field around the fatigue crack for a nickel single crystal and for a copper single crystal, Fig. 5e–h, during various loading cycles. The characteristics of fatigue crack growth in both nickel and copper are similar in most of the orientations, with some noticeable differences for orientation *B*. This orientation indicates that copper single crystal (Fig. 5f) exhibits a strong tendency to form microcracks at directions oriented to 45° with the horizontal direction [010], enlarging the main crack to a void-like shape. In the case of nickel (Fig. 5b), the propagation mechanism involves the creation of small voids in the crack plane and linkage with the main crack. Orientations *A* and *D* show that in both cases of nickel (Fig. 5a) and copper (Fig. 5e), the crack tip plastic zone is mainly double slip. Orientation *C* for both nickel (Fig. 5c) and copper (Fig. 5g) indicates that the crack propagates as

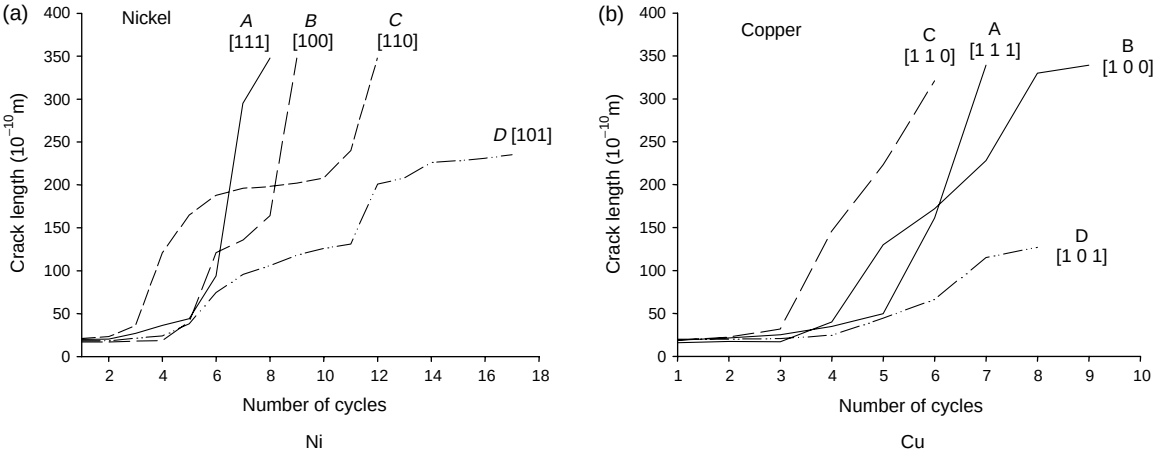

Fig. 6. Variation of total crack length with number of cycles. Comparison between different crystal orientations.

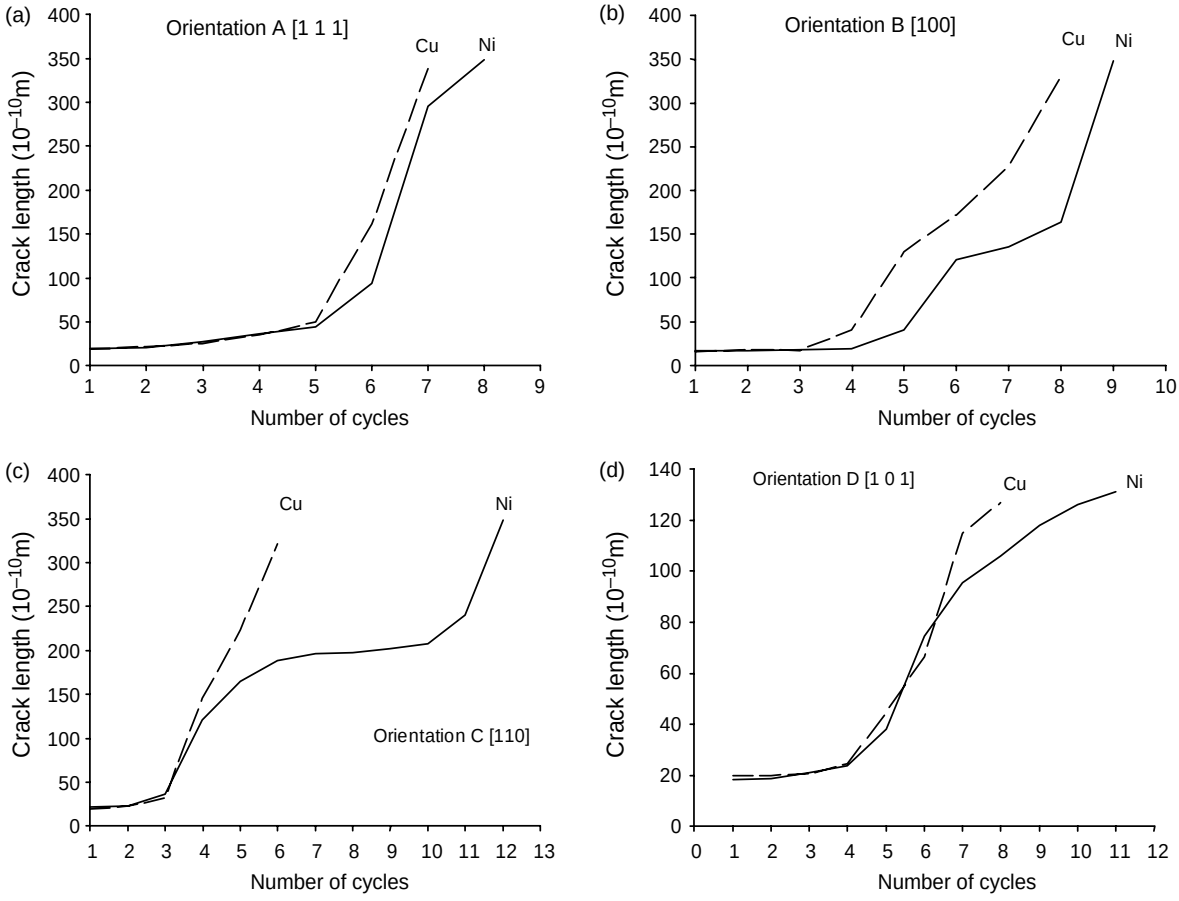

Fig. 7. Comparison of crack growth with number of cycles between nickel and copper single crystals for each orientation *A–D*.

mode I crack with a very small crack tip blunting much different than orientation *B*. Another interesting feature is that the orientation *D* (Fig. 5d) for nickel does not experience crack deviation into mixed mode I+ II like in case of variable amplitude loading.

Comparison between all orientations for nickel and copper are shown in Fig. 6. The results indicate that the crack growth rate is highly dependent on orientation for both crystals. For the first 6 cycles when the crack is small, and it did not enter yet the zone w the edge effect is dominant, the largest crack growth rate is experienced by the orientation *C* [110]. In this case, the rapid crack growth can be associated with the very little crack tip blunting observed. The smallest crack growth rate for both nickel and copper is shown by orientation *D* [101]. By comparing the crack growth rates of individual orientation in Fig. 7 it can be observed that constantly copper exhibits crack growth rates larger that Ni.

The strain rate applied to the specimens in all simulations was 2×10^{9}/sec. This represents a high strain rate value, especially when fatigue loading is under investigation, and it is due to the inherent nature of molecular dynamics simulations. A study of the influence of the applied strain rate on crack growth rate was performed by considering various strain rates analyzed 10^{8}/sec–10^{9}/sec, and the results are shown in Fig. 8. All strain rates analyzed indicated no significant differences on the crack growth rate during the steady state regime, when the cracks are not influenced by the edges of the specimen. However, as the crack grows to a point where the crack tip is in the vicinity of the specimen edge,

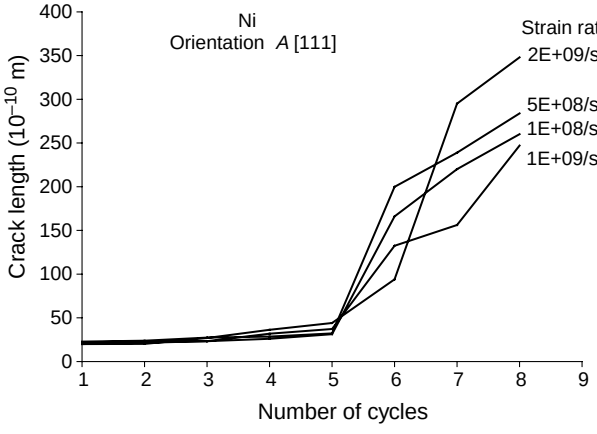

Fig. 8. Influence of strain rate on fatigue crack growth.

differences in the growth rates under different strain rates were observed.

6. Conclusions

Fatigue damage by persistent slip band formation, cyclic stress–strain curves, and crack growth were simulated using molecular dynamics in nickel and copper single crystals. The formation of shear bands is highly dependent on the crystal orientation. Significant directions on the stereographic triangle indicated that the dislocation structure during the fatigue loading vary from double and triple slip, to veins that form in planes parallel with the $[\bar{1}10]$ direction. The stress hardening for nickel single crystal fatigues at constant strain amplitude of 5×10^{-3} and 0.5 load ratio indicated a sudden increase due to major dislocation bands formation. The orientation was shown not to play a major role in determining at which cycle this sudden stress hardening occurred.

Fatigue crack growth simulation at increasing strain amplitude (in nickel) and constant strain amplitude (in nickel and copper) were performed and the mechanisms of crack advance were studied. When the loading was oriented in the [111] direction, both nickel and copper experienced double slip structures with the shear bands symmetrically oriented with respect to the loading direction. The third shear band along $[\bar{1}10]$ observed in the case of fatigued nickel near a small circular void, was not observed very significantly in the crack growth simulations, however, the crack maintained a planar configuration, propagating along this third shear direction. [100] orientation revealed a planar crack propagation in the case of nickel with small voids nucleating in front of the crack and coplanar with the crack, while copper single crystals experienced void nucleation at 45° from the horizontal direction around the crack tip. In the [110] orientation the void formation is not significant for the fatigue crack propagation mechanisms. The crack tip does not have significant blunting, and the propagation mechanism involves mainly tearing of atomic bond in the crack plane at the crack tip. For this orientation, the crack advance is very rapid compared with other orientations, especially in the first six cycles when the influence of the specimen edges are not significant. Orientation [101] indicated for both nickel and copper the smallest amount of crack growth. The crack tip experienced an evident double slip pattern with consequential shear bands in the vicinity of the crack. By performing a comparative analysis, it was also observed that for all conditions (geometry, loading, crystal orientation) similar, cracks propagated more rapidly in copper that in nickel single crystals.

References

[1] Mayer H, Laird C. Frequency effects on cyclic plastic strain of polycrystalline copper under variable loading. Mater Sci Eng A 1995; 194:137–45.
[2] Thompson N, Wadsworth N, Louat, N. The origin of fatigue fracture in copper. Philos Mag 1955;1:113–126.
[3] Jin NY. Dislocation structures in fatigued copper single crystals oriented for double slip. Philos Mag A 1983;48(5):L33–L8.
[4] Cheng AS, Laird C. Fatigue life behavior of copper single crystals. Part I. Observations of crack nucleation. Mater Sci Eng 1981;4(4):331–41.
[5] Helgeland O. Cyclic hardening and fatigue of copper single crystals. J Inst Metals 1965;93:570–4.
[6] Mughrabi H. The cyclic hardening and saturation behavior of copper single crystals. Mater Sci Eng 1978;33:207–23.
[7] Lorenzo F, Laird C. Strain bursts in pure copper subjected to various forms of static and cyclic loading at ambient temperature. Mater Sci Eng 1982;52:187–94.
[8] Zhang ZF, Wang ZG, Sun ZM. Evolution and microstructural characteristics of deformation bands in fatigued copper single crystals. Acta Mater 2001;49:2875–86.
[9] Basinski ZS, Pascual R, Basinski SJ. Low amplitude fatigue of copper single crystals. I. The role of the surface in fatigue failure. Acta Metall 1983;1(4):591–602.
[10] Buque C. Dislocation structures and cyclic behavior of [011] and $[\bar{1}11]$-oriented nickel single crystals. Int J Fatigue 2001;23:671–8.
[11] Bhat S, Laird C. High temperature cyclic deformation of nickel. Fatigue Eng Mater Struct 1979;1:59–77.
[12] Bhat S, Laird C. High temperature cyclic deformation of DS-nickel. Fatigue Eng Mater Struct 1979;1:79–92.
[13] Shen Y-L. On the atomistic simulation of plastic deformation and fracture in crystals. J Mater Res 2004;19(4):973–6.
[14] Inoue H, Akahoshi Y, Harada S. Molecular dynamics simulation on fracture mechanisms of nano-scale polycrystal under static and cyclic loading. Mater Sci Res Int 1995;1(2):95–100.
[15] Heino P, Hakkinen H, Perondi L, Kaski K. Molecular dynamics study of copper and aluminum under mechanical strain. Mater Res Soc Symp Proc 1999;539:245–50.
[16] Baskes MI, Johnson RA. Modified embedded atom potentials for HCP metals. Model Simul Mater Sci Eng 1994;2:147–63.
[17] Baskes MI. The modified embedded atom method. Comput Mater Model 1994;294:23–35. AD-Vol. 42/PVP.
[18] Baskes MI. Determination of modified embedded atom method parameters for nickel. Mater Chem Phys 1997;50:152–8.
[19] Daw MS, Baskes MI. Embedded-atom method: derivation and application to impurities, surfaces, and other defects in metals. Phys Rev B 1984;29:6443.
[20] Horstemeyer MF. From atoms to autos. A new design paradigm using microstructure-property modeling. Part 1. Monotonic loading. Sandia National Laboratories, SAND2000-8662 2001.